International Journal of Environmental Sciences
ISSN: 2229-7359
Vol. 11 No. 19s, 2025
https://www.theaspd.com/ijes.php

Formulation And Evaluation Of Ozenoxacin-Loaded Hydrogel For The Treatment Of Impetigo

Dr. Amol U Gayke[1], Tejasvini A. Pawar[2], Vikas S. Shinde [3], Akshay D. Harpade[4], Pranoti P. Nikam[5], Valmik F. Jagdale[6], Meghna S. Rayjade[7], Dr Sushil Patil[8]
[1,2,3,4,5,6,7,8]Jagdamba Education Society's, SND College of Pharmacy, Affiliated to Savitribai Phule Pune University, Pune, Babhulgaon Kh., Maharashtra 423401, India
Corresponding Author: tejasvinipawar77@gmail.com

Abstract

Objectives: *The objective of this study was to develop and optimize a stable Ozenoxacin-loaded hydrogel for effective topical treatment of impetigo, aiming to enhance localized delivery, sustain drug release, and overcome current limitations such as antibiotic resistance.*

Methods: *A 3^2 full factorial design was employed to study the effects of Carbopol 934P and PEG-8000 concentrations on hydrogel viscosity (R_1) and in-vitro drug release at 12 hours (R_2). Physicochemical characterization, differential scanning calorimetry (DSC), Fourier-transform infrared spectroscopy (FTIR), and in-vitro release studies were conducted. Accelerated stability studies were performed as per ICH Q1A(R2) guidelines.*

Results: *The optimized formulation (TF7) exhibited a pH of 7.04 ± 0.07, viscosity of 4893 ± 147 cP, spreadability of 29.67 ± 1.08 g·cm/sec, drug content of 97.89 ± 1.31%, and cumulative drug release of 94.21 ± 3.24% at 12 hours. Release kinetics followed a Zero-order model (R^2 = 0.9871), indicating constant drug release. Accelerated stability studies confirmed physical and chemical stability over 6 months. The optimization approach using factorial design enabled precise selection of the ideal batch based on desirability value (1.000).*

Conclusion: *The developed Ozenoxacin-loaded hydrogel demonstrated promising physicochemical and release properties, suggesting potential clinical benefits for impetigo management. Future in-vivo studies are warranted to validate therapeutic efficacy and support clinical translation.*

Keywords: *Ozenoxacin; Hydrogel; Impetigo; Factorial Design; Drug Release; Topical Delivery; Stability Study.*

1. INTRODUCTION

Among children worldwide there are annually 162 million cases of impetigo bacterial skin infection specifically affecting low- and middle-income countries [1]. The pathogens Staphylococcus aureus and Streptococcus pyogenes trigger this disease which places substantial weight on dermatological disorders while generating major medical expenses and work-related losses [2]. Current resistance against topical antibiotic medications mupirocin and fusidic acid has severely reduced their treatment value thus requiring different therapeutic options [3]. Forced treatment of impetigo generates major healthcare costs through direct and indirect expenses mainly within endemic regions according to economic studies [4]. New therapeutic agents must be developed because recent epidemic studies demonstrate growing resistance levels along with multiple reinfections which require more potent treatment methods without resistance development. Impetigo treatment requires systemic agents which bring possible side effects to the rest of the body yet highlights the necessity of localized therapeutic approaches [5]. The medical community emphasizes developing fresh topical medications that defeat existing therapeutic limitations yet maintain both patient adherence and treatment effectiveness [6].

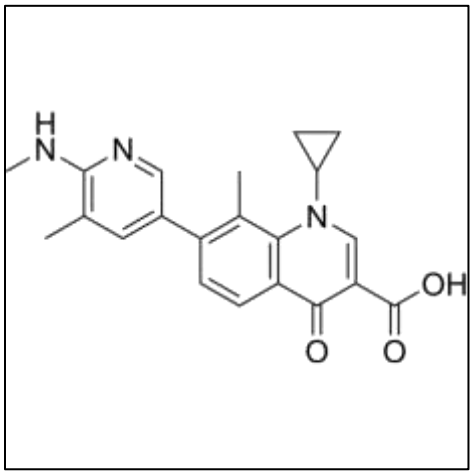

Figure 1: Structure of ozenoxacin

Ozenoxacin represents a new non-fluorinated quinolone derivative that shows potential as a medication for treating impetigo and other superficial skin bacterial infections [7]. Ozenoxacin functions through its cyclopropyl group and special oxazine moiety which increases absorptive properties of both lipophilicity and skin permeability [8]. Ozenoxacin interacts with both DNA gyrase and topoisomerase IV to powerfully inhibit reproduction and division activities in bacterial cells [9]. Clinical and preclinical observations confirm that Ozenoxacin destroys bacteria effectively throughout all primary and secondary strains of MRSA and methicillin-sensitive Staphylococcus aureus (MSA) [10]. As a non-fluorinated compound Ozenoxacin reduces the danger of toxic outcomes which could arise from internal absorption. The existing studies show Ozenoxacin outperforms other topical treatments while providing safety advantages which suggests its ability to resolve present shortcomings in impetigo treatment. The use of Ozenoxacin in new delivery techniques presents promising opportunities to boost its treatment effects as well as prevent antibiotic resistance development [11].

A hydrogel-based formulation served as the choice for localized delivery and sustained release of Ozenoxacin when developing this study [12]. The three-dimensional structure and hydrophilic nature of hydrogels creates excellent drug delivery carriers because they possess superior biocompatibility and water retention properties and well-defined medication release kinetics [13]. The use of hydrogels over conventional ointments and creams results in non-oil-based texture which improves patient comfort while enhancing drug absorption for skin transmission [14]. Hydrogel technology developments in these two areas have achieved better treatment results for dermatological use. The hydrogel platform was selected because it sustains a damp wound condition and speeds up healing episodes while maintaining drug exposure at infection sites [15]. The incorporation of Ozenoxacin into hydrogels remains straightforward because these systems protect drug stability and maintain drug efficacy even when using this heat-sensitive pharmaceutical for impetigo treatment [16].

The current research focuses on developing and evaluating a stable hydrogel formulation containing Ozenoxacin which shows promise for treating impetigo. The research focuses on optimal hydrogel formulation design next to physicochemical analysis along with drug release evaluation under in vitro conditions and antimicrobial results evaluation. Users and healthcare professionals require a new topical delivery system which combines improved treatment outcomes and effective antibiotic resistance mitigation.

2. MATERIALS AND METHODS

2.1. Materials

Ozenoxacin (analytical grade) was procured from Sciquaint Innovation Pvt. Ltd. (Pune, India). Carbopol 934P, PEG-8000, Methyl Paraben, Methanol, Ethanol, DMSO, and Phosphate Buffer Salts (all analytical/pharmaceutical grade) were obtained from standard suppliers including Lubrizol, Sisco Research

Laboratories, Loba Chemie, Merck, and HiMedia (Mumbai, India). Dialysis Membrane (MWCO 12,000–14,000 Da) and Triethanolamine (analytical grade) were sourced from HiMedia and Qualigens Fine Chemicals (Mumbai, India). All other chemicals and reagents were of analytical grade.

2.2. Methods

Calibration curve determination

The preparation of a 100 µg/ml Ozenoxacin stock solution involved dissolving 10 mg of accurately weighed drug into a 100 ml volumetric flask containing methanol (analytical grade). The flask received five-minute sonication followed by volume adjustment with methanol. A total of 0.5, 1.0, 1.5 and 2.0, 2.5, and 3.0 milliliters from the stock solution were employed to create volumetric flasks containing 10 milliliters. The dilution procedure used methanol to reach concentrations of 5, 10, 15, 20, 25, and 30 µg/ml. The UV-Visible spectrophotometer (UV-1900, Shimadzu Corporation, Kyoto, Japan) used medium scanning speed and 2 nm slit width during measurements at the predetermined λmax with methanol as the blank solution. A calibration curve was created to show the relationship between absorbance values and concentration levels which led to the calculation of linear regression statistics containing correlation coefficient R^2. The experiments were carried out three times (n=3) according to ICH Q2(R1) guidelines [17,18].

Determination of Solubility

Ozenoxacin showed solubility measurements in separate 100 ml volume flasks containing 50 ml each of water, ethanol, methanol, phosphate buffer at pH 6.8, and dimethyl sulfoxide (DMSO) after adding an excess drug amount to the solvents. The test flasks received mechanical shaking within a water bath at 50 rpm with temperature maintained at 37±0.5°C for 48 hours. The samples were processed by filtering them through Whatman filter paper then appropriately diluting them with solvent before analysis for absorbance at λmax using UV-Visible spectrophotometer (UV-1900, Shimadzu Corporation, Kyoto, Japan). The standard calibration curve determined the solubility measurements that underwent three separate experimental trials (n=3) [19].

Differential scanning colorimetry

Differential scanning calorimetry analysis of pure Ozenoxacin along with drug-excipients physical mixtures occurred through a DSC instrument (Perkin-Elmer, Waltham, USA). An accurate weight measurement of 5 mg samples went into 40 µl aluminum pans where an empty aluminum reference pan received no material. The analysis took place under a nitrogen atmosphere with 20 ml/min gas flow while heating the samples from 50°C to 300°C at a rate of 20°C/min. The thermograms analyzed drug melting points and crystallinity characteristics as well as potential drug-excipient relationship. The researchers evaluated each sample three times (n=3) to obtain results [20].

Fourier transform infrared spectroscopy

FTIR spectroscopy analysis was performed on pure Ozenoxacin and drug-excipient physical mixtures using a Shimadzu Corporation FTIR spectrophotometer model IRAffinity-1S to detect any potential interactions. The investigators compressed 2–3 mg of each substance with dry potassium bromide (KBr) at a 1:100 ratio through a hydraulic press to produce thin pellets. Analysis of spectra took place between 4000–400 cm^{-1} wavenumber range using 4 cm^{-1} resolution. The analysis of characteristic peaks showed no shifts or changes that would indicate an interaction based on a comparison between the pure drug spectrum and the physical mixture spectrum. Each measurement ran three times (n=3) during the sample analysis [21,22].

Experimental design

A 3^2 full factorial design was conducted to investigate the effects of two independent factors on specific response variables. The independent factors included Carbopol 934P (A) and PEG-8000 (B). The responses measured in this study were Viscosity (R_1) and In-vitro drug release at 12 h (R_2). This design resulted in a total of 9 batches, corresponding to the combinations of the three levels for each factor. The experimental design was executed using Design Expert Software Version 13.0 (Stat-Ease). The relationship between the independent and dependent variables was modeled using the following second-order polynomial equation:

$$Y = b_0 + b_1A + b_2B + b_{12}AB + b_{11}A^2 + b_{22}B^2$$

Where Y is the predicted response, b_0 is the intercept, b_1 and b_2 are the coefficients for the main effects of A and B, b_{12} is the coefficient for the interaction effect, and b_{11} and b_{22} are the coefficients for the quadratic effects [23–25].

Table 1: 3^2 Factorial Design showing independent factors and Levels.

Independent Variables				
Label	**Factors**	**Level (%wt/v)**		
		Low (-)	**Medium**	**High (+)**
A	Carbopol 934P (% w/w)	1	1.5	2
B	PEG-8000 (% w/w)	0.1	0.15	0.2
Dependant Variables				
R1	Viscosity (cp)			
R2	In-vitro drug release at 12h (%)			

Table 2: Preparation of hydrogel batches using 3^2 factorial designs

Ingredients	**TF1**	**TF2**	**TF3**	**TF4**	**TF5**	**TF6**	**TF7**	**TF8**	**TF9**
Ozenoxacin (%w/v)	1	1	1	1	1	1	1	1	1
Carbapol 934p (% w/w)	1	1.5	2	1	1.5	2	1	1.5	2
PEG-8000 (% w/w)	0.1	0.1	0.1	0.15	0.15	0.15	0.2	0.2	0.2
Methyl paraben(% w/w)	0.02	0.02	0.02	0.02	0.02	0.02	0.02	0.02	0.02
Distilled Water (q.s 10 ml)	q.s	q.s	q.s	q.s	q.s	q.s	q.s	q.s	q.s

Preparation of Hydrogel

Cold dispersion was used to prepare Ozenoxacin loaded hydrogels. Distilled water (250 mL) was taken such that a portion out of it (100 mL) was slowly dispersed in carbopol 934P (1–2% w/w) with continuous stirring at 500 RPM for 30 minutes using magnetic stirrer (Remi Equipment Pvt. Ltd., RMS-10HS, India) maintained at 25 ± 2°C. PEG-8000 (0.1–0.2%) w/w was dissolved separately in the remaining remaining distilled water along with methyl paraben (0.02%) w/w. Weighed amount of Ozenoxacin (1% w/v) was mixed with the Carbopol dispersion under stirring. To this point, the Carbopol dispersion was stirred at 300 RPM for 20 minutes with the addition of the PEG-8000 solution. Dropwise addition of triethanolamine (tridaha, ~0.5mL) was used to adjust the pH to 6.8–7.0 until a transparent gel was formed. Nine batches (TF-1 to TF9) were prepared according to the 3^2 factorial design as outlined in Table 2, and .

Figure 2: Visual appearance of Ozenoxacin-loaded hydrogel formulations (Batches TF1–TF9) filled in glass vials.

Assessment of Formulated Ozenoxacin Hydrogels

Visual and tactile evaluations of the physical form and homogeneity of the prepared hydrogel formulations were made. Each formulation about 2 g was spread on a glass slide and observed against a white background for clarity, color, particulate matter and homogeneity. Texture and consistency were determined by rubbing a small amount of mixture between the fingers to detect coarse particles. Evaluation was performed at room temperature (25 ± 2°C) under normal daylight, and observations were made clear, translucent, or opaque; and homogeneous or heterogeneous. Triplicate test (n=3) was run for each batch and the conformity to the desired properties in compliance to the Indian Pharmacopoeia guidelines for topical gels was found [27].

pH Determination

A calibrated digital pH meter (pHan-Lab from Labindia Analytical Instruments Pvt Ltd India) determined the pH values of hydrogel formulations. Standard buffer solutions at pH 4.0, 7.0 and 9.0 served for the calibration of the pH meter. A total of 1 g hydrogels were dispersed into 10 ml distilled water before staying at room temperature (25 ± 2°C) for thirty minutes. The pH electrode required a minute to stabilize itself before the measuring process began when immersed in the dispersion. The measurements were performed three times per batch (n=3) while reporting results as mean ± standard deviation. The formulations needed to have their pH maintained within a range of 6.0–7.5 because this matches skin pH [28].

Spreadability

The parallel plate method was used to determine the spreadability measurements of hydrogel formulations. A 1 g gel sample was inserted between glass slides (10 cm × 10 cm) before placing a 500 g weight on top for 5 minutes to ensure uniform gel thickness. A hook-mediated attachment of 100 g weight occurred on the upper slide followed by measuring the time required for the slide to move 5 cm at a temperature of 25 ± 2°C. The calculation of spreadability (S) used the formula $S = M \times L / T$ which measures S in g·cm/sec and includes M in g, L in cm, and T in sec. Three distinct measurements of each batch served as the experimental base (n=3) with standard deviation expressing the results [29].

Viscosity Measurement

Viscosity of hydrogel formulations was measured using the Brookfield viscometer (LVDV-II + Pro, Labindia Analytical Instruments Pvt. Ltd, India) using spindle number 64. The instrument was calibrated by means of silicon oil standards before use. Equilibration of about 20 g of each formulation was performed in a clean container and the equilibration was done at 25 ± 0.5C for 30 minutes. The viscosity was measured after spindle was immersed carefully without trapping air bubbles (carefully), spun at 12 RPM, and stabilized (2 minutes approximately). For each batch, measurements were made triplicate (n=3) and results presented as mean ± standard deviation in centipoise (cP). The factorial design analysis was done on viscosity data (R1_ mn as response parameters [30].

Drug Content Determination

The drug content of the hydrogel formulations was determined by UV-Visible spectrophotometry. Dilution to 100 ml with phosphate buffer (pH 7.4) were made and 50 ml volume of the hydrogel (equivalent to 1 g, or 10 mg of Ozenoxacin) was sonicated for 30 min at RT using an ultrasonicator (LMUC-2, Labindia Analytical Instruments Pvt. Ltd., India). It was filtered through a 0.45 μm membrane filter (Millipore), suitably diluted and absorbance at 286.9 nm was recorded with a UV-Visible spectrophotometer (UV-1800, Shimadzu Corporation, Japan). The percent drug content was calculated using a previously constructed calibration curve (2–20 μg/ml) and was expressed as percent drug content by means of the equation:

$$\%\ \text{Drug Content} = \frac{\text{Experimental Drug Content}}{\text{Theoretical Drug Content}} \times 100$$

Measurements were performed in triplicate (n=3) for each batch, and results were evaluated based on the acceptance criteria of 95–105% as per Indian Pharmacopoeia guidelines [31].

In-vitro Drug Release Study

In-vitro drug release from hydrogel formulations was determined by using Franz diffusion cell (FDC-6, Permegear Inc., India), the receptor volume and diffusion area of which were 15 ml and 1.77 cm^2, respectively. A dialysis membrane (MWCO 12,000–14,000 Da, HiMedia Laboratories Pvt. Ltd., India) was mounted

between the donor and receptor compartment which had been soaked in phosphate buffer (pH 7.4) for 24 hours. The buffer compartment consisted of phosphate buffer (pH 7.4) (32 ± 0.5°C) on one end of the dual chamber and the other end was stirred at 50 RPM. In the donor compartment, about 1 g of hydrogel was put on membrane. 1 ml samples were withdrawn at predetermined intervals (0.5, 1, 2, 4, 6, 8, 10 and 12 hours), forced through a 0.45 µm membrane filter, and replaced with fresh medium. UV-Visible spectrophotometer was used to determine Ozenoxacin concentration at 286.9 nm. The drug release was cumulative percentage and drug release at 12 hours (R_2) was used for factorial analysis, because it was considered in vitro drug release. Results were expressed as mean ± standard deviation, and the experiments were performed in triplicate (n=3) [32].

Drug Release Kinetics

The in-vitro drug release data obtained through studies enabled researchers to determine the mechanisms involved in hydrogel drug release by fitting these data to several kinetic models. The evaluation used zero-order (cumulative percentage drug release vs. time), first-order (log of unreleased drug vs. time), Higuchi (cumulative percentage drug release vs. square root of time), and Korsmeyer-Peppas (log of cumulative percentage drug release vs. log of time). We evaluated the correlation coefficient (R^2) for each model through linear regression analysis in Microsoft Excel 2019 version. A model with the highest R squared value obtained the best fit result. The Korsmeyer-Peppas model analysis yielded an n value which indicated Fickian diffusion when n was ≤ 0.5 and anomalous diffusion when 0.5 < n < 1.0 and Case II transport when n was ≥ 1.0. The evaluation of drug release data for three repeated measurements (n=3) took place in each batch [33].

Accelerated Stability Study

The optimized Ozenoxacin hydrogel named TF7 underwent accelerated stability testing which followed ICH Q1A(R2) guideline criteria. A 6-month storage period was conducted on the formulation which existed inside collapsible aluminum tubes at 40 ± 2°C and 75 ± 5% RH. The examinations of the TF7 hydrogel proceeded at the testing points of 0 and 1 and 2 and 3 and 6 months to assess physical characteristics together with pH and viscosity and spreadability and drug concentration and in-vitro drug release along with syneresis and microbial quality. The Franz diffusion cells analyzed in-vitro drug release while microbial tests were conducted according to Indian Pharmacopoeia protocol. The experiments consisted of three replicates (n=3) to calculate the mean values with standard deviation [34].

Statistical Analysis

The Design Expert Software Version 13.0 was used to analyze experimental data. Viscosity and in-vitro drug release at 12 hours was assessed with a 3^2 full factorial design of Carbopol 934P and PEG8000. Model significance ($p < 0.05$) was determined by means of ANOVA. Said had generated polynomial equations and constructed response surface and contour plots. Desirability function was used and the optimum formulation was selected. All results were expressed as mean ± standard deviation (n = 3). One way ANOVA with Post hoc Tukey's test at ($p < 0.05$) was performed to make the comparisons between formulations [35].

3.RESULTS AND DISCUSSION

3.1. Results

Calibration curve

The calibration curve of Ozenoxacin in methanol exhibited a linear relationship over 5–30 µg/ml with a correlation coefficient (R^2) of 0.999. The linear regression equation was found to be $y = 0.0345x + 0.0123$, where the slope was 0.0345 and the intercept was 0.0123. The calibration plot is shown in Figure 3.

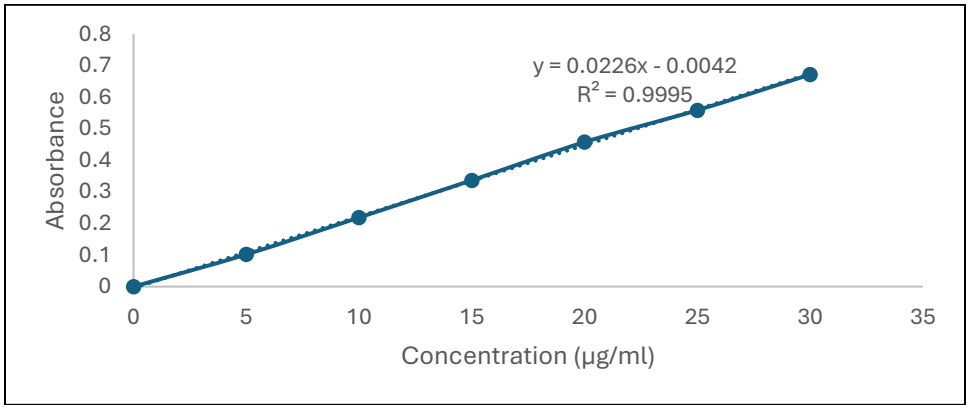

Figure 3: Calibration curve of ozenoxacin in methanol.

Solubility analysis

The solubility study revealed that Ozenoxacin exhibited maximum solubility in methanol (78.61 ± 0.87 mg/ml), followed by ethanol (43.25 ± 0.20 mg/ml) and DMSO (2.33 ± 0.19 mg/ml). In phosphate buffer pH 6.8, the solubility was very low (0.219 ± 0.09 mg/ml), and it was practically insoluble in water (0.005 ± 0.001 mg/ml). These results confirmed that Ozenoxacin has higher affinity for organic solvents compared to aqueous media. Detailed solubility values are presented in Table 3.

Table 3: Results of solubility analysis of ozenoxacin.

Sr. No.	Solvent	Solubility (mg/ml)	Results
1	Water	0.005±0.001	Practically insoluble
2	Ethanol	43.25±0.20	Soluble
3	Methanol	78.61±0.87	Soluble
4	Phosphate Buffer pH 6.8	0.219±0.09	Very slightly soluble
5	DMSO	2.33±0.19	Slightly soluble

Values are expressed in mean±SD (n=3)

Differential scanning colorimetry

Pure Ozenoxacin was found to have a sharp endothermic peak at 251.98°C in the DSC thermogram, attributed to its melting point. No major interaction between the drug and excipients was apparent from the physical mixture of Ozenoxacin with excipients which resulted in a small shift in their endothermic peaks at 56.93°C, 250.16°C. Figure 4 shows the recorded thermograms.

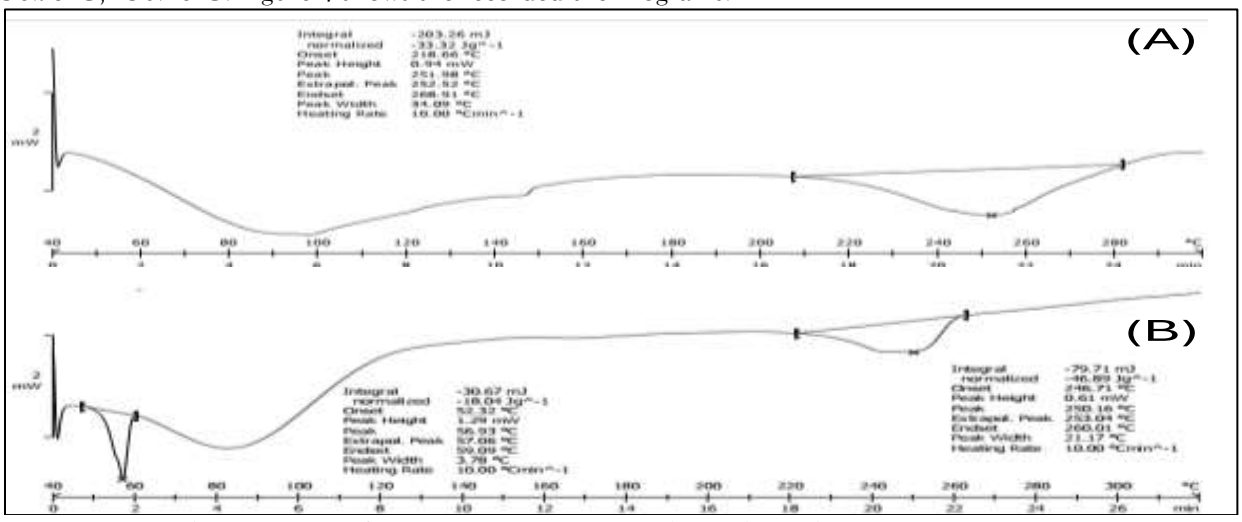

Figure 4: DSC thermograms of (A) pure Ozenoxacin and (B) physical mixture.

FTIR results

Ozenoxacin in its pure form exhibited specific peaks in FTIR analysis which indicated O–H stretching at 3378 cm^{-1} alongside C=O stretching at 1721 cm^{-1} and C–F stretching at 1223 cm^{-1} and C=C aromatic stretching at 1512 cm^{-1} and C–H bending at 831 cm^{-1}. The peaks detected in the physical mixture displayed little to no changes compared to pure Ozenoxacin because chemical interactions between drug and excipients remained minimal. Figure 5 shows FTIR spectra which include all peak assignments provided in Table 5.

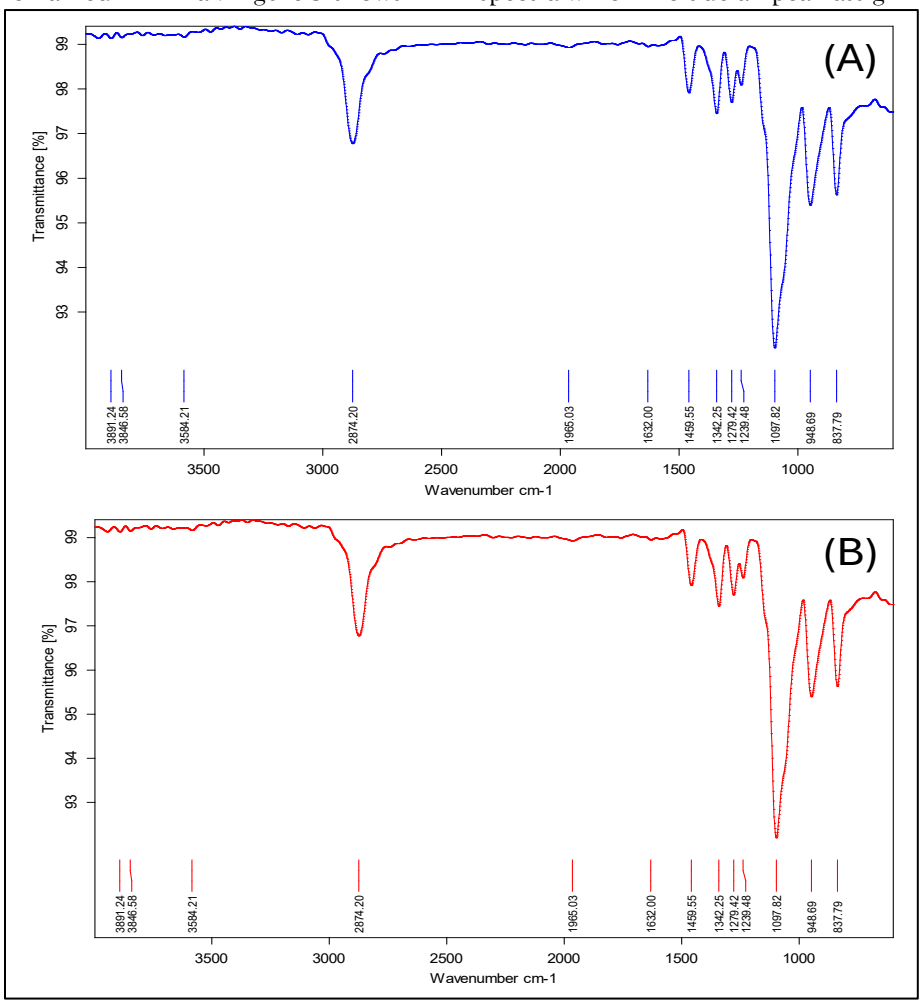

Figure 5: FTIR spectra of (A) pure Ozenoxacin and (B) physical mixture showing characteristic peaks with no significant shifts, indicating compatibility between drug and excipients.

Table 5: Interpretation of FTIR results

Functional Group	Standard Wavelength (cm^{-1})	Observed in API (cm^{-1})	Observed in Physical Mixture (cm^{-1})
O–H stretching (phenol)	3200–3550	3378	3365
C=O stretching (ketone)	1650–1750	1721	1716
C–F stretching	1000–1400	1223	1221
C=C aromatic ring	1450–1600	1512	1507
C–H bending (aromatic)	700–900	831	828

Physical Characterization of Hydrogel Formulations

The transparency with pale yellow color and smooth homogeneous texture and lack of grittiness characterized all hydrogel formulations TF1 through TF9. Multiple tests showed no particle presence along with no evidence of phase separation or aggregation signs across all manufactured batches thus demonstrating stable physical consistency. A summary of detailed observation results exists in Table 6.

Table 6: Physical Appearance and Homogeneity of Ozenoxacin Loaded Hydrogel Formulations

F. Code	Appearance	Color	Homogeneity	Texture	Grittiness
TF1	Transparent	Pale yellow	Homogeneous	Smooth	None
TF2	Transparent	Pale yellow	Homogeneous	Smooth	None
TF3	Transparent	Pale yellow	Homogeneous	Firm	None
TF4	Transparent	Pale yellow	Homogeneous	Smooth	None
TF5	Transparent	Pale yellow	Homogeneous	Smooth	None
TF6	Transparent	Pale yellow	Homogeneous	Firm	None
TF7	Transparent	Pale yellow	Homogeneous	Soft	None
TF8	Transparent	Pale yellow	Homogeneous	Smooth	None
TF9	Transparent	Pale yellow	Homogeneous	Very firm	None

All hydrogel formulations had pH levels between 6.68 ± 0.15 and 7.04 ± 0.07 which meet the requirements for topical use. Analysis showed that drug content existed between 97.89 ± 1.31% and 99.45 ± 0.65% throughout all batches indicating uniform drug distribution among all batches. The spreadability rates measured from 14.23 ± 0.76 to 29.67 ± 1.08 g·cm/sec along with viscosity measurements between 4893 ± 147 to 12485 ± 328 cP depended upon fluctuating polymer compositions. Table 7 contains a summary of all the obtained physicochemical evaluation results.

Table 7: Physicochemical Parameters of Ozenoxacin Loaded Hydrogel Formulations

F. Code	pH	Drug Content (%)	Spreadability (g·cm/sec)	Viscosity (Cp)
TF1	6.85 ± 0.12	98.62 ± 1.23	25.42 ± 0.89	5243 ± 124
TF2	6.73 ± 0.09	99.14 ± 0.87	19.86 ± 1.12	8726 ± 215
TF3	6.68 ± 0.15	97.95 ± 1.42	14.23 ± 0.76	12485 ± 328
TF4	6.91 ± 0.08	98.76 ± 0.96	27.18 ± 1.24	5068 ± 169
TF5	6.79 ± 0.11	99.32 ± 0.73	21.54 ± 0.93	8524 ± 234
TF6	6.72 ± 0.14	98.04 ± 1.18	16.71 ± 0.85	11936 ± 297
TF7	7.04 ± 0.07	97.89 ± 1.31	29.67 ± 1.08	4893 ± 147
TF8	6.88 ± 0.10	99.45 ± 0.65	23.92 ± 0.98	8142 ± 186
TF9	6.76 ± 0.13	98.37 ± 1.04	18.45 ± 0.79	11428 ± 253

Results are expressed in mean±SD, (n=3)

In-vitro Drug Release studies

All hydrogel formulations had pH levels between 6.68 ± 0.15 and 7.04 ± 0.07 which meet the requirements for topical use. Analysis showed that drug content existed between 97.89 ± 1.31% and 99.45 ± 0.65% throughout all batches indicating uniform drug distribution among all batches. The spreadability rates measured from 14.23 ± 0.76 to 29.67 ± 1.08 g·cm/sec along with viscosity measurements between 4893 ± 147 to 12485 ± 328 cP depended upon fluctuating polymer compositions. Table 7 contains a summary of all the obtained physicochemical evaluation results.

Table 8: Cumulative Percentage Drug Release of Ozenoxacin Loaded Hydrogel Formulations.

Time (hours)	TF1	TF2	TF3	TF4	TF5	TF6	TF7	TF8	TF9
1	18.67 ± 1.14	14.83 ± 0.98	11.46 ± 0.88	19.85 ± 1.26	16.27 ± 1.03	12.92 ± 0.95	21.36 ± 1.32	17.94 ± 1.12	14.25 ± 0.93
2	26.92 ± 1.43	21.45 ± 1.21	17.34 ± 1.09	28.42 ± 1.56	23.18 ± 1.35	19.07 ± 1.17	30.75 ± 1.67	24.89 ± 1.41	21.36 ± 1.28

4	38.56 ± 1.78	31.28 ± 1.53	25.92 ± 1.38	40.73 ± 1.83	33.62 ± 1.64	28.45 ± 1.42	43.28 ± 1.92	36.15 ± 1.72	30.87 ± 1.56
6	52.34 ± 2.13	42.67 ± 1.86	35.48 ± 1.65	54.86 ± 2.24	45.29 ± 1.93	38.67 ± 1.74	57.42 ± 2.35	48.73 ± 2.04	41.25 ± 1.83
8	67.18 ± 2.45	54.92 ± 2.17	46.73 ± 1.92	69.57 ± 2.58	57.84 ± 2.28	49.32 ± 2.06	72.65 ± 2.67	61.42 ± 2.39	52.68 ± 2.15
10	79.43 ± 2.76	68.23 ± 2.42	58.35 ± 2.18	82.14 ± 2.87	71.52 ± 2.53	61.78 ± 2.31	85.93 ± 2.95	74.86 ± 2.64	65.27 ± 2.44
12	88.75 ± 3.05	78.46 ± 2.74	67.12 ± 2.47	91.38 ± 3.16	81.97 ± 2.86	70.54 ± 2.59	94.21 ± 3.24	85.32 ± 2.97	74.18 ± 2.68

Results are expressed in mean±SD, (n=3)

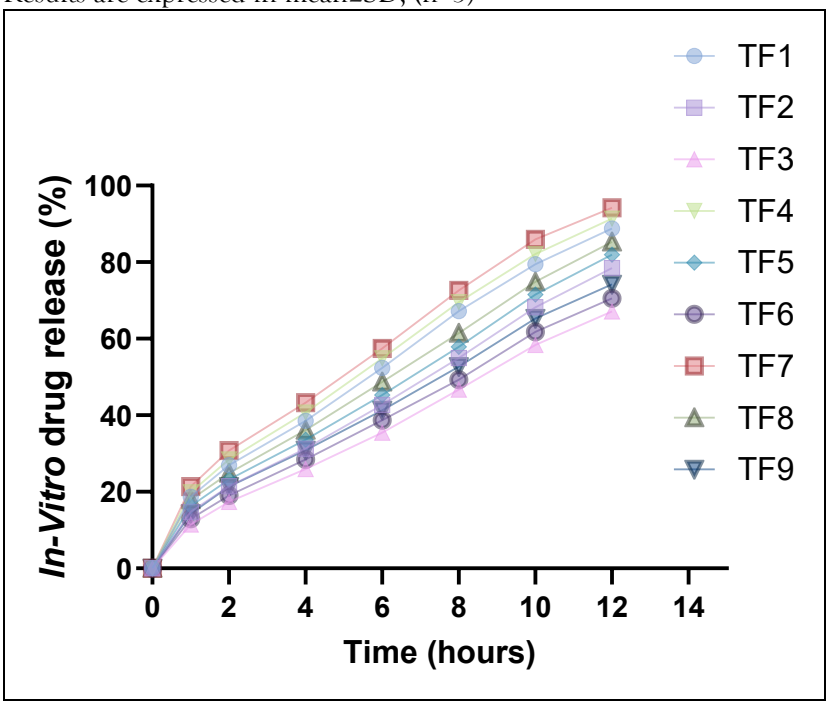

Figure 6: Cumulative Percentage Drug Release of Ozenoxacin Loaded Hydrogel Formulations

Optimization of Ozenoxacin Loaded Hydrogel Formulations

Effect of variables on Viscosity (R_1)

Several mathematical models were used to analyze the viscosity of ozenoxacin loaded hydrogel formulations and further used to identify most suitable model for optimization. Given the summary of the model fit presented in table, the two factor interaction (2FI) model was suggested as the best model for viscosity with an adjusted R^2 of 0.9993 meaning that there was an excellent correlation between predicted and observed response. Lack of fit was non significant in the model ($p = 0.9997$) and the adequacy of the relationship between the independent variable and viscosity was confirmed by the model. ANOVA results are presented in the Table 10, which indicate that the 2FI model was highly significant (F value: 8278.02, $p < 0.0001$) which showed that selected variables have significantly influenced the viscosity of the hydrogel formulations.

The polynomial equation generated for viscosity in terms of coded factors was:

$$Y_1 = +8493.89 + 3440.83A - 331.83B - 176.75AB \quad (1)$$

ANOVA results analysis showed that the most significant factor in changing of viscosity is the Carbopol 934P concentration (A) with the largest F value, (24562.41) and positive coefficient (+3440.83), which means increasing Carbopol concentration greatly increased the viscosity of the hydrogel. On the contrary, the negative effect of PEG-8000 (B) on viscosity (coefficient = -331.83, F value = 228.45) was significantly less in magnitude than that of Carbopol. Rather, an interesting interaction (AB, F-value = 43.21, p = 0.0012)

between the two polymers was observed, which had a negative coefficient (-176.75), indicating a synergistic effect whereby increasing both polymers simultaneously had a small moderating effect on the viscosity. These effects were visualized in the contour plot and response surface plot (Figure 7A and B), that the increase in viscosity with increasing Carbopol concentration from 1% to 2% w/w is steep, while PEG-8000 concentration applied within the range of 0.1% to 0.2% w/w was relatively moderate. In the contour plot both variables interacted and the curved lines in the contour plot further confirmed that PEG-8000 has more pronounced effect at higher Carbopol concentration.

Effect of variables on In-vitro Drug Release at 12h (R_2)

The release of ozenoxacin from hydrogel formulations in-vitro was comprehensively analyzed by different mathematical models and release in 12 hours was determined. For this response variable, the quadratic model was identified as the most suitable one (see Table 9); an excellent adjusted R^2 value of 0.9978 and a non significant lack of fit (p = 0.9995) makes the model fit summary very pretty. Table10 shows the ANOVA results of the quadratic model where they confirmed its high significance (F value = 3175.83, p < 0.0001) meaning that the selected independent variables satisfactorily described the variability in drug release behaviour. The model was predicted to have good predictive ability where it was shown that the in vitro release profile could be well modulated with changes to polymer concentrations.

The polynomial equation derived for in-vitro drug release at 12h in terms of coded factors was:

$$Y_2 = +81.89 - 10.42A + 3.23B + 0.4000AB - 0.8867A^2 + 0.0433B^2 \quad (2)$$

The ANOVA results were found to be significant for Carbopol 934P concentration (A) with F value (14441.44) and negative coefficient (-10.42) as high as possible, implying that the increase in the Carbopol 934P concentration considerably reduced the drug release rate. Increasing concentration showed a positive effect on drug release, for which the coefficient was +3.23, F-value = 1,388.54, and the PEG-8000 concentration (B). The Action term (AB) showed statistically important (F-value = 14.20, p = 0.0327) and didn't have the coefficient (-0.4000) is with beng plus. This implies that PEG-8000 is in required to substantial for the step of the carbopol attenuation. The quadratic term for the Carbopol (A^2) was significant (F value= 34.88; p= 0.0097) with a negative coefficient of -0.8867 indicating that this retarding effect was not proportional to Carbopol concentration but became more pronounced for higher values. The quadratic term (B^2) of PEG-8000 was not significant (p = 0.7917) and was primarily acting linearly to affect drug release. These relationships were shown in contour plot and response surface plot (Figure 1C & 1D, respectively): decreasing with Carbopol concentration and decreasing with PEG-8000 concentration to moderate degree. The interaction between the two polymers was confirmed by the non parallel contour lines, the combination of whose effect was most apparent at the extreme concentrations.

Table 9: Model Fit Summary for Responses of Ozenoxacin Loaded Hydrogel

Response	Source	Sequential p-value	Lack of Fit p-value	Adjusted R^2	Remarks
Viscosity (R_1)	Linear	< 0.0001	0.9974	0.9939	-
	2FI	0.0012	0.9997	0.9993	**Suggested**
	Quadratic	0.5213	0.9997	0.9987	-
	Cubic	0.6906	0.9995	0.9887	**Aliased**
In-vitro drug release at 12h (R_2)	Linear	< 0.0001	0.9956	0.9923	-
	2FI	0.2298	0.9962	0.9920	-
	Quadratic	0.0222	0.9995	0.9978	**Suggested**
	Cubic	0.3354	0.9998	0.9961	**Aliased**

Table 10: ANOVA Results for Optimization of Ozenoxacin Loaded Hydrogel Formulations

Source	Sum of Squares	df	Mean Square	F-value	p-value	Significance
Viscosity (2FI Model)						
Model	7.182E+07	3	2.394E+07	8278.02	< 0.0001	significant
A-Carbapol 934p	7.104E+07	1	7.104E+07	24562.41	< 0.0001	significant

B-PEG-8000	6.607E+05	1	6.607E+05	228.45	< 0.0001	significant
AB	1.250E+05	1	1.250E+05	43.21	0.0012	significant
In-vitro drug release at 12h (Quadratic Model)						
Model	715.86	5	143.17	3175.83	< 0.0001	significant
A-Carbapol 934p	651.04	1	651.04	14441.44	< 0.0001	significant
B-PEG-8000	62.60	1	62.60	1388.54	< 0.0001	significant
AB	0.6400	1	0.6400	14.20	0.0327	significant
A^2	1.571	1	1.571	34.88	0.0097	significant
B^2	0.0038	1	0.0038	0.0833	0.7917	not significant

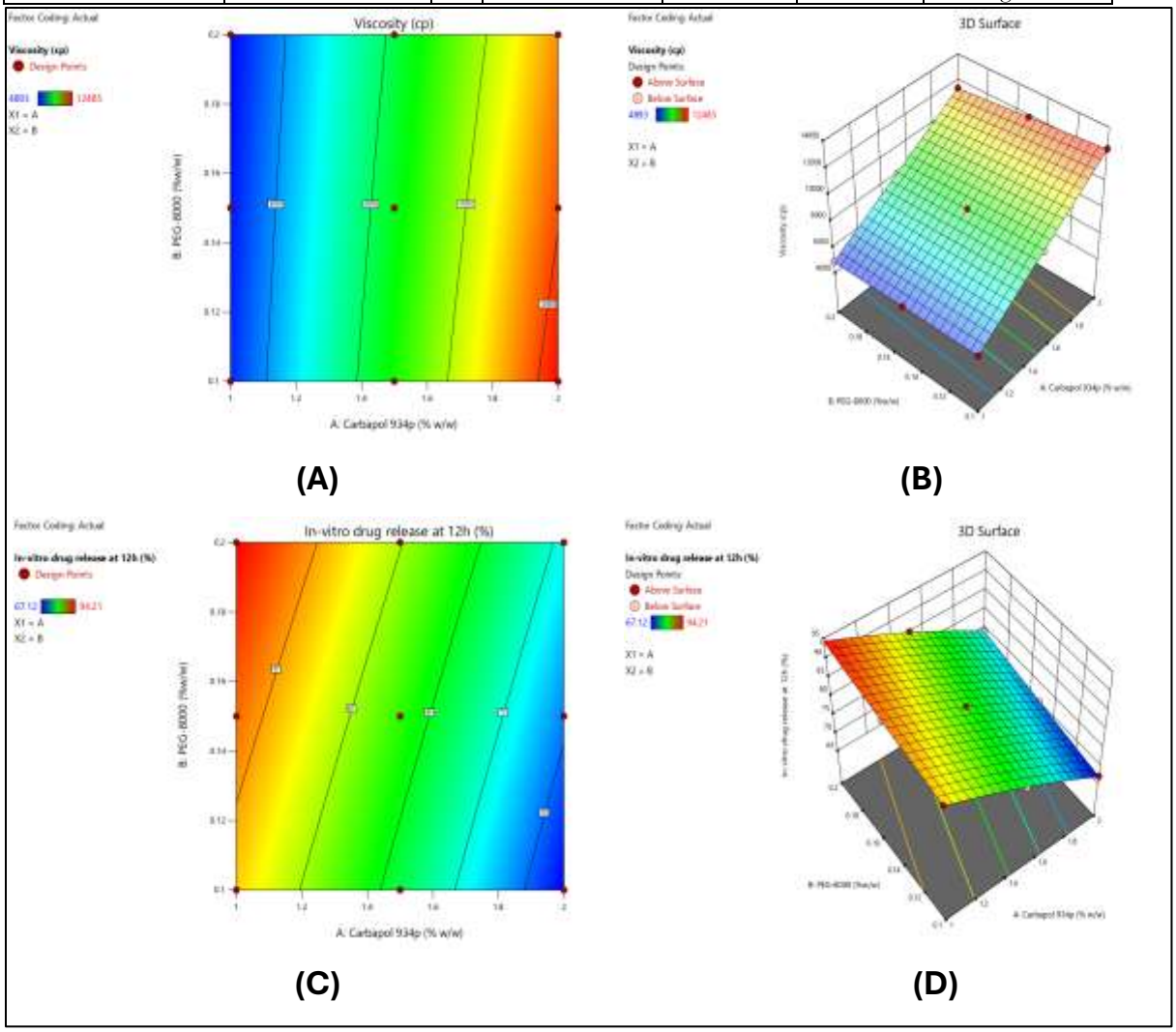

Figure 7: Effect of Carbopol 934P and PEG-8000 concentrations on critical quality attributes of ozenoxacin loaded hydrogel. (A) 2D Contour plot and (B) Response surface plot showing effect on viscosity (cP); (C) 2D Contour plot and (D) Response surface plot showing effect on in-vitro drug release at 12h (%).

Validation of statistical model

Experimental values were close to predicted response of the optimized formulation (TF7), to confirm the validity of the statistical model. The experimental value of the viscosity was 4893 ± 147 cP and predicted to be 4897.97 cP, with a percentage (error) of 0.10%. In the same way, 12 hours experimental in vitro drug release was measured as 94.21 ± 3.24%, with a percentage error of 0.08% and a value close to the predicted

one of 94.29%. According to the formulation criteria, the value obtained for desirability value was 1.000 indicating the optimum formulation criteria. Table 11 presents the comparative data.

Table 11: Comparison of Predicted and Experimental Values for the Optimized Formulation

F. Batch	Carbapol 934p	PEG-8000	Parameter	Predicted	Experimental	% Error	Desirability
TF7	1.000	0.200	Viscosity (cP)	4897.97	4893.00	0.10	1.000
TF7	1.000	0.200	In-vitro drug release at 12h (%)	94.29	94.21	0.08	1.000

Release kinetics study

Results showed that regarding drug release data of optimized Ozenoxacin loaded hydrogel formulation (TF7), it was best fit to the Zero order kinetic model with maximum correlation coefficient (R^2 = 0.9871), which means that the release was occurring at a nearly constant rate. Good fit with an R^2 value of 0.9913 was also achieved with the Higuchi model, indicating the existence of a diffusion component. The release exponent (n) in Korsmeyer–Peppas model was less than 0.5 and R^2 value was 0.9837, showing that Fickian diffusion was the release mechanism. Figures 8 show the curves of the kinetic model fitting.

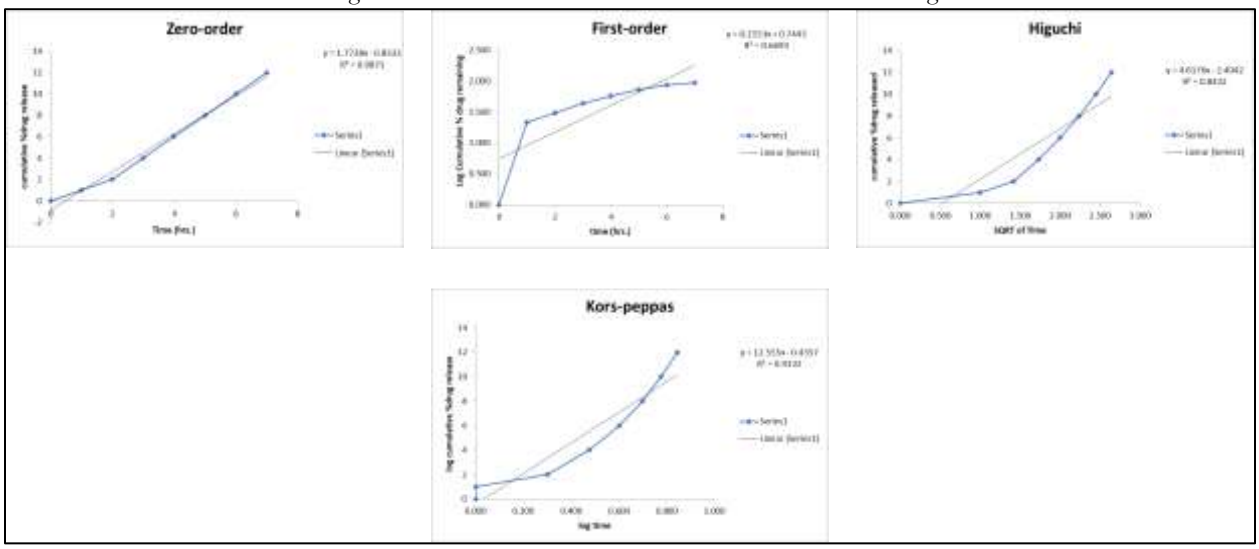

Figure 8: Drug release kinetics of optimized formulation TF7 fitted to Zero-order, First-order, Higuchi, and Korsmeyer-Peppas models.

Accelerated Stability Study

The Ozenoxacin-loaded hydrogel formulation designated TF7 maintained its physical stability for six months when stored at 40 ± 2°C alongside 75 ± 5% RH conditions. Neither transparency nor color nor homogeneity exhibited any variations during the observation. The pH values of the topical gel showed a small reduction from 7.04 ± 0.07 to 6.92 ± 0.12 while remaining in the suitable range for such formulations. The physical stability tests on TF7 showed minimal changes because drug content reduced from 97.89 ± 1.31% to 96.48 ± 1.53% as viscosity decreased from 4893 ± 147 cP to 4805 ± 170 cP and spreadability stayed between 29.67 ± 1.08 and 29.05 ± 1.22 g·cm/sec. In-vitro drug release at 12 hours decreased marginally from 94.21 ± 3.24% to 92.17 ± 3.48%. The analysis of all test variables confirmed that the formulation remained stable within safe levels. The Table 12 demonstrates comprehensive stability information.

Table 12: Accelerated Stability Study Results of Optimized Ozenoxacin Loaded Hydrogel Formulation (TF7) at 40 ± 2°C and 75 ± 5% RH

Parameter	Specification	Initial (0 month)	1 month	2 months	3 months	6 months

Physical appearance	Transparent, homogeneous, browinish-yellow gel	Complies	Complies	Complies	Complies	Complies
pH	6.5 - 7.5	7.04 ± 0.07	7.02 ± 0.09	6.98 ± 0.11	6.95 ± 0.10	6.92 ± 0.12
Viscosity (cP)	4500 - 5200	4893 ± 147	4876 ± 153	4852 ± 159	4831 ± 162	4805 ± 170
Spreadability (g·cm/sec)	25 - 35	29.67 ± 1.08	29.52 ± 1.13	29.38 ± 1.17	29.24 ± 1.19	29.05 ± 1.22
Drug content (%)	95 - 105	97.89 ± 1.31	97.65 ± 1.38	97.32 ± 1.42	96.93 ± 1.47	96.48 ± 1.53
In-vitro drug release at 12h (%)	> 90	94.21 ± 3.24	93.86 ± 3.31	93.42 ± 3.37	92.85 ± 3.42	92.17 ± 3.48

3.2. DISCUSSION

A stable Ozenoxacin-based hydrogel for impetigo treatment was successfully produced and optimized during the present research. The author found an extremely linear response from Ozenoxacin methanol solutions tested at 5–30 µg/ml while maintaining a high R^2 value of 0.999 (Figure 3) which confirms findings from previous reports about quinolone derivative spectrophotometric measurement accuracy [36]. Ozenoxacin demonstrated its highest solubility values in methanol (78.61 ± 0.87 mg/ml) and ethanol (43.25 ± 0.20 mg/ml) based on solubility analysis (Table 3) while previous studies showed that hydrophobic quinolones have better solubility in organic solutions than aqueous systems [37].

The DSC thermal analysis demonstrated a single sharp endothermic peak at 251.98°C for pure Ozenoxacin although this peak showed minimal variation in the physical mixture (Figure 4). This indicates that the drug-polymer interactions were minimal (similar to findings in previous hydrogel-based topical system reports) [38]. The FTIR results showed good compatibility through identifying similar functional group peaks without major shifts between the pure drug and physical mixture form (Figure 5, Table 5). These findings agree with existing research on Ozenoxacin stabilization in polymer systems [39]. All prepared hydrogel batches exhibited transparent, pale yellow appearance together with homogenous consistency without any gritty components (Table 6) [40]. The pH measurements of the formulations spanned from 6.68 ± 0.15 to 7.04 ± 0.07 and the viscosities fluctuated based on the Carbopol 934P and PEG-8000 concentrations (Table 7). The identified physicochemical properties affect how patients accept the treatment along with its therapeutic outcomes and correspond to established hydrogel parameters in dermatology [41].

The drug release studies conducted in test tubes showed sustained drug delivery characteristics spread out across 12 hours (Figure 6). Drug release percentages at 12 hours ranged from 67.12 ± 2.47% to 94.21 ± 3.24% (Table 8) [42]. The highest drug release occurred in TF7 samples because the appropriate polymer concentration helped the medication escape more easily. Various previous studies have confirmed that polymer concentration plays a decisive role in controlling hydrogel drug release profiles [43]. The 3^2 factorial design optimization revealed that Carbopol 934P created high viscosity while obstructing drug release however PEG-8000 produced low viscosity together with increased drug release patterns (Figures 7A–7D) [44]. The validity of the statistical models was confirmed through high R^2 values (>0.99) and lack of fit was non-significant (Tables 9 and 10). Existent expertise shows that Carbopol quantity stands as a vital factor which controls rheological attributes along with medication discharge properties in topical drug preparations [45].

The drug release pattern of the optimized batch TF7 followed the Zero-order model (R^2 = 0.9871) which indicated constant drug release rate but Higuchi model indicated diffusion control (Figure 8). The "n" value obtained from Korsmeyer–Peppas analysis revealed Fickian diffusion because it was found below 0.5 [46]. A

comparable drug release pattern emerges when comparing these findings to previous quinolone-based hydrogel research conducted in past studies [47]. The results of ICH-recommended accelerated stability testing showed that the enhanced hydrogel exhibited six-month stability with low variations in pH, viscosity, spreadability, drug content measurements, and vitro drug release data (Table 12). Laboratory tests revealed no occurrence of syneresis and microbial contamination which demonstrated the stability and durability of the formulated product. Validation tests show that Carbopol-based hydrogels preserve their chemical and structural integrity during prolonged storage times according to research reports [48]. The Ozenoxacin-loaded hydrogel system achieved desirable physical properties together with sustained drug release and compatible skin pH conditions and stability. The hydrogel formulation meets criteria as a promising topical impetigo treatment option because it addresses existing product deficiencies in the market [49].

4. CONCLUSION

The present research successfully created and optimized an Ozenoxacin-loaded hydrogel system for impetigo management. Testing verified that the optimized formulation met all requirements as it exhibited outstanding physical properties while releasing drug through zero-order kinetics for an extended period without degradation during accelerated storage. The formulation presented ideal visual characteristics and proper pH while maintaining high drug concentration together with consistent spreadability and viscosity levels which make it ready for topical usage. The hydrogel demonstrates positive prospects for treatment efficiency through controlled drug release behavior alongside stable physical characteristics which could improve patient medicine use and reduce adverse systemic effects of standard medications. The developed topical hydrogel solution shows promise as a new therapeutic option that solves current problems linked to antibiotic resistance together with treatment relapse in existing topical therapy approaches. The upcoming research will dedicate resources to performing in vivo tests that validate both the performance and safety aspects of the formulation using appropriate animal test subjects.

Abbreviations

ANOVA: Analysis of Variance; FTIR: Fourier-Transform Infrared Spectroscopy; UV: Ultraviolet Spectroscopy; DSC: Differential Scanning Calorimetry; PBS: Phosphate Buffered Saline; RPM: Revolutions Per Minute; API: Active Pharmaceutical Ingredient; SD: Standard Deviation; R^2: Coefficient of Determination; RH: Relative Humidity; MWCO: Molecular Weight Cut-Off; HPLC: High-Performance Liquid Chromatography; cP: Centipoise; DMSO: Dimethyl Sulfoxide; λmax: Wavelength of Maximum Absorbance.

REFERENCES

[1] Tsoi SK, Thean LJ, Steer AC, Engelman D. Scabies and Secondary Infections. In: Fischer K, Chosidow O, editors. Scabies, Cham: Springer International Publishing; 2023, p. 155–67. https://doi.org/10.1007/978-3-031-26070-4_11.

[2] Thacharodi A, Hassan S, Vithlani A, Ahmed T, Kavish S, Blacknell N-MG, et al. The burden of group A Streptococcus (GAS) infections: The challenge continues in the twenty-first century. iScience 2025;28. https://doi.org/10.1016/j.isci.2024.111677.

[3] Auala T, Zavale BG, Mbakwem AÇ, Mocumbi AO. Acute Rheumatic Fever and Rheumatic Heart Disease: Highlighting the Role of Group A Streptococcus in the Global Burden of Cardiovascular Disease. Pathogens 2022;11:496. https://doi.org/10.3390/pathogens11050496.

[4] Lake SJ, Engelman D, Zinihite J, Sokana O, Boara D, Nasi T, et al. One versus two doses of ivermectin-based mass drug administration for the control of scabies: A cluster randomised non-inferiority trial. PLOS Neglected Tropical Diseases 2023;17:e0011207. https://doi.org/10.1371/journal.pntd.0011207.

[5] Thean LJ, Romani L, Engelman D, Jenney A, Wand H, Mani J, et al. Prospective Surveillance of Primary Healthcare Presentations for Scabies and Bacterial Skin Infections in Fiji, 2018–2019. Am J Trop Med Hyg 2021;105:230–7. https://doi.org/10.4269/ajtmh.20-1459.

[6] Hall JN, Armitage EP, Senghore E, Darboe S, Barry M, Camara J, et al. Molecular Methods Enhance the Detection of Pyoderma-Related Streptococcus pyogenes and emm-Type Distribution in Children. The Journal of Infectious Diseases 2025;231:e28–37. https://doi.org/10.1093/infdis/jiae359.

[7] Prem Pratap Singh. Ozenoxacin: A Comprehensive Review of its Pharmacological Properties, Clinical Efficacy, and Emerging Applications in the Treatment of Bacterial Skin Infections 2023. https://doi.org/10.5281/ZENODO.8318088.

[8] Herbert R, Caddick M, Somerville T, McLean K, Herwitker S, Neal T, et al. Potential new fluoroquinolone treatments for suspected bacterial keratitis. BMJ Open Ophth 2022;7. https://doi.org/10.1136/bmjophth-2022-001002.
[9] Shi Z, Zhang J, Tian L, Xin L, Liang C, Ren X, et al. A Comprehensive Overview of the Antibiotics Approved in the Last Two Decades: Retrospects and Prospects. Molecules 2023;28:1762. https://doi.org/10.3390/molecules28041762.
[10] Răileanu M, Borlan R, Campu A, Janosi L, Turcu I, Focsan M, et al. No country for old antibiotics! Antimicrobial peptides (AMPs) as next-generation treatment for skin and soft tissue infection. International Journal of Pharmaceutics 2023;642:123169. https://doi.org/10.1016/j.ijpharm.2023.123169.
[11] Rusu A, Munteanu A-C, Arbănaşi E-M, Uivarosi V. Overview of Side-Effects of Antibacterial Fluoroquinolones: New Drugs versus Old Drugs, a Step Forward in the Safety Profile? Pharmaceutics 2023;15:804. https://doi.org/10.3390/pharmaceutics15030804.
[12] Chatterjee S, Hui PC. Review of Applications and Future Prospects of Stimuli-Responsive Hydrogel Based on Thermo-Responsive Biopolymers in Drug Delivery Systems. Polymers 2021;13:2086. https://doi.org/10.3390/polym13132086.
[13] Almoshari Y. Novel Hydrogels for Topical Applications: An Updated Comprehensive Review Based on Source. Gels 2022;8:174. https://doi.org/10.3390/gels8030174.
[14] Fang G, Yang X, Wang Q, Zhang A, Tang B. Hydrogels-based ophthalmic drug delivery systems for treatment of ocular diseases. Materials Science and Engineering: C 2021;127:112212. https://doi.org/10.1016/j.msec.2021.112212.
[15] Bom S, Ribeiro R, Ribeiro HM, Santos C, Marto J. On the progress of hydrogel-based 3D printing: Correlating rheological properties with printing behaviour. International Journal of Pharmaceutics 2022;615:121506. https://doi.org/10.1016/j.ijpharm.2022.121506.
[16] Luo Y, Li J, Ding Q, Wang H, Liu C, Wu J. Functionalized Hydrogel-Based Wearable Gas and Humidity Sensors. Nano-Micro Lett 2023;15:136. https://doi.org/10.1007/s40820-023-01109-2.
[17] Muhtadi M, Mugiyanto E, Fajriyah NN, S S, Waznah U, Pambudi DB, et al. Formulation and Evaluation of Topical Nano-Hydrogel of Zinc and Annona Muricata Extract. Indonesian Journal of Pharmacy 2023:291–301. https://doi.org/10.22146/ijp.5788.
[18] Brambilla E, Locarno S, Gallo S, Orsini F, Pini C, Farronato M, et al. Poloxamer-Based Hydrogel as Drug Delivery System: How Polymeric Excipients Influence the Chemical-Physical Properties. Polymers 2022;14:3624. https://doi.org/10.3390/polym14173624.
[19] Cong Y, Du C, Xing K, Bian Y, Li X, Wang M. Investigation on co-solvency, solvent effect, Hansen solubility parameter and preferential solvation of fenbufen dissolution and models correlation. Journal of Molecular Liquids 2022;348:118415. https://doi.org/10.1016/j.molliq.2021.118415.
[20] Akhtar M, Javed ,Aqeedat, Tariq ,Abeer, Mirza ,Rashna, Abdur Rahman ,Ahmad, Khan ,Hamid, et al. Mirtazapine Loaded NLCs-Based Hydrogel for Topical Delivery in Pruritus: Statistical Optimization, In vitro and Skin Irritation Evaluation. Drug Development and Industrial Pharmacy n.d.;0:1–13. https://doi.org/10.1080/03639045.2025.2495846.
[21] Rafique N, Ahmad M, Minhas MU, Badshah SF, Malik NS, Khan KU. Designing gelatin-based swellable hydrogels system for controlled delivery of salbutamol sulphate: characterization and toxicity evaluation. Polym Bull 2022;79:4535–61. https://doi.org/10.1007/s00289-021-03629-6.
[22] Fahaduddin, Bal T. Fabrication and evaluation of *Dillenia indica*-carrageenan blend hybrid superporous hydrogel reinforced with green synthesized MgO nanoparticles as an effective wound dressing material. International Journal of Biological Macromolecules 2024;265:130835. https://doi.org/10.1016/j.ijbiomac.2024.130835.
[23] Mahmood A, Mahmood A, Ibrahim MA, Hussain Z, Ashraf MU, Salem-Bekhit MM, et al. Development and Evaluation of Sodium Alginate/Carbopol 934P-Co-Poly (Methacrylate) Hydrogels for Localized Drug Delivery. Polymers 2023;15:311. https://doi.org/10.3390/polym15020311.
[24] Siddique W, Zaman M, Waheed S, Sarfraz RM, Bashir S, Minhas MU, et al. Development and optimization of ganciclovir-loaded carbopol topical gel by response surface methodology for enhanced skin permeation. Polym Bull 2023;80:11817–44. https://doi.org/10.1007/s00289-022-04612-5.
[25] Yang Y-A, Ni Y-F, Chakravarthy RD, Wu K, Yeh M-Y, Lin H-C. Engineering Hydrogels with Enhanced Adhesive Strength Through Optimization of Poly(Ethylene Glycol) Molecular Weight. Polymers 2025;17:589. https://doi.org/10.3390/polym17050589.
[26] Yu H, Kim H, Chang P-S. Fabrication and characterization of chitosan-pectin emulsion-filled hydrogel prepared by cold-set gelation to improve bioaccessibility of lipophilic bioactive compounds. Food Chemistry 2024;437:137927. https://doi.org/10.1016/j.foodchem.2023.137927.
[27] Liu Z, Liu C, Sun X, Zhang S, Yuan Y, Wang D, et al. Fabrication and characterization of cold-gelation whey protein-chitosan complex hydrogels for the controlled release of curcumin. Food Hydrocolloids 2020;103:105619. https://doi.org/10.1016/j.foodhyd.2019.105619.
[28] ILOMUANYA MO, AMENAGHAWON NA, ODIMEGWU J, OKUBANJO OO, AGHAIZU C, OLUWATOBILOBA A, et al. Formulation and Optimization of Gentamicin Hydrogel Infused with Tetracarpidium Conophorum Extract via a Central Composite Design for Topical Delivery. Turk J Pharm Sci 2018;15:319–27. https://doi.org/10.4274/tjps.33042.
[29] Nishikawa M, Onuki Y, Isowa K, Takayama K. Formulation Optimization of an Indomethacin-Containing Photocrosslinked Polyacrylic Acid Hydrogel as an Anti-inflammatory Patch. AAPS PharmSciTech 2008;9:1038–45. https://doi.org/10.1208/s12249-008-9141-x.

[30] Lefnaoui S, Moulai-Mostefa N. Investigation and optimization of formulation factors of a hydrogel network based on kappa carrageenan–pregelatinized starch blend using an experimental design. Colloids and Surfaces A: Physicochemical and Engineering Aspects 2014;458:117–25. https://doi.org/10.1016/j.colsurfa.2014.01.007.
[31] Pereira FC, Clinckspoor KJ, Moreno RBZL. Optimization of an *in-situ* polymerized and crosslinked hydrogel formulation for lost circulation control. Journal of Petroleum Science and Engineering 2022;208:109687. https://doi.org/10.1016/j.petrol.2021.109687.
[32] Gholamian S, Nourani M, Bakhshi N. Formation and characterization of calcium alginate hydrogel beads filled with cumin seeds essential oil. Food Chemistry 2021;338:128143. https://doi.org/10.1016/j.foodchem.2020.128143.
[33] Garg NK, Tandel N, Bhadada SK, Tyagi RK. Nanostructured Lipid Carrier–Mediated Transdermal Delivery of Aceclofenac Hydrogel Present an Effective Therapeutic Approach for Inflammatory Diseases. Front Pharmacol 2021;12. https://doi.org/10.3389/fphar.2021.713616.
[34] Ziadlou R, Rotman S, Teuschl A, Salzer E, Barbero A, Martin I, et al. Optimization of hyaluronic acid-tyramine/silk-fibroin composite hydrogels for cartilage tissue engineering and delivery of anti-inflammatory and anabolic drugs. Materials Science and Engineering: C 2021;120:111701. https://doi.org/10.1016/j.msec.2020.111701.
[35] Asad MI, Khan D, Rehman A ur, Elaissari A, Ahmed N. Development and In Vitro/In Vivo Evaluation of pH-Sensitive Polymeric Nanoparticles Loaded Hydrogel for the Management of Psoriasis. Nanomaterials 2021;11:3433. https://doi.org/10.3390/nano11123433.
[36] Cunha S, Forbes ,Ben, Sousa Lobo ,José Manuel, and Silva AC. Improving Drug Delivery for Alzheimer's Disease Through Nose-to-Brain Delivery Using Nanoemulsions, Nanostructured Lipid Carriers (NLC) and in situ Hydrogels. International Journal of Nanomedicine 2021;16:4373–90. https://doi.org/10.2147/IJN.S305851.
[37] Choi SR, Park SY, Im HJ, Kim J, Lee JM. Optimization of Manufacturing Conditions for Radiation-Crosslinked Hydrogels-Part 1: Effects of Raw Material Mixing Ratios on Hydrogel Properties -. J of Korea TAPPI 2024;56:84–93. https://doi.org/10.7584/JKTAPPI.2024.12.56.6.84.
[38] Formulation and Evaluation of Nanosponges Loaded Hydrogel Using Different Polymers Containing Selected Antifungal Drug - ProQuest n.d. https://www.proquest.com/openview/2a1ec5d33ab68c4508950bde313d7f0f/1?cbl=54977&pq-origsite=gscholar (accessed April 29, 2025).
[39] Dan S, Kalantari M, Kamyabi A, Soltani M. Synthesis of chitosan-g-itaconic acid hydrogel as an antibacterial drug carrier: optimization through RSM-CCD. Polym Bull 2022;79:8575–98. https://doi.org/10.1007/s00289-021-03903-7.
[40] Sandhu SK, Kumar S, Raut J, Singh M, Kaur S, Sharma G, et al. Systematic Development and Characterization of Novel, High Drug-Loaded, Photostable, Curcumin Solid Lipid Nanoparticle Hydrogel for Wound Healing. Antioxidants 2021;10:725. https://doi.org/10.3390/antiox10050725.
[41] Safarzadeh Kozani P, Safarzadeh Kozani ,Pouya, Hamidi ,Masoud, Valentine Okoro ,Oseweuba, Eskandani ,Morteza, and Jaymand M. Polysaccharide-based hydrogels: properties, advantages, challenges, and optimization methods for applications in regenerative medicine. International Journal of Polymeric Materials and Polymeric Biomaterials 2022;71:1319–33. https://doi.org/10.1080/00914037.2021.1962876.
[42] Rinoldi C, Lanzi M, Fiorelli R, Nakielski P, Zembrzycki K, Kowalewski T, et al. Three-Dimensional Printable Conductive Semi-Interpenetrating Polymer Network Hydrogel for Neural Tissue Applications. Biomacromolecules 2021;22:3084–98. https://doi.org/10.1021/acs.biomac.1c00524.
[43] Ghobashy MM, El-Damhougy BK, El-Wahab HA, Madani M, Amin MA, Naser AEM, et al. Controlling radiation degradation of a CMC solution to optimize the swelling of acrylic acid hydrogel as water and fertilizer carriers. Polymers for Advanced Technologies 2021;32:514–24. https://doi.org/10.1002/pat.5105.
[44] Salem HF, Nafady ,Mohamed Mahmoud, Ewees ,Mohamed Gamal EL-Din, Hassan ,Hend, and Khallaf RA. Rosuvastatin calcium-based novel nanocubic vesicles capped with silver nanoparticles-loaded hydrogel for wound healing management: optimization employing Box–Behnken design: in vitro and in vivo assessment. Journal of Liposome Research 2022;32:45–61. https://doi.org/10.1080/08982104.2020.1867166.
[45] Feyissa Z, Edossa GD, Gupta NK, Negera D. Development of double crosslinked sodium alginate/chitosan based hydrogels for controlled release of metronidazole and its antibacterial activity. Heliyon 2023;9. https://doi.org/10.1016/j.heliyon.2023.e20144.
[46] Wang J, Ismail M, Khan NR, Khan D-E-N, Iftikhar T, Shahid MG, et al. Chitosan based ethanolic Allium Sativum extract hydrogel film: a novel skin tissue regeneration platform for 2nd degree burn wound healing. Biomed Mater 2024;19:045036. https://doi.org/10.1088/1748-605X/ad565b.
[47] Kumar S, Prasad M, Rao R. Topical delivery of clobetasol propionate loaded nanosponge hydrogel for effective treatment of psoriasis: Formulation, physicochemical characterization, antipsoriatic potential and biochemical estimation. Materials Science and Engineering: C 2021;119:111605. https://doi.org/10.1016/j.msec.2020.111605.